

(NASA-CR-195870) A LINEARIZED
DYNAMIC MODEL OF THE LARGE-ANGLE
MAGNETIC SUSPENSION TEST FIXTURE
(Old Dominion Univ.) 19 p

N94-71974

Unclass

Z9/09 0008619

NAG-1-1056

A LINEARIZED DYNAMIC MODEL of the LARGE-ANGLE MAGNETIC SUSPENSION TEST FIXTURE

Colin P. Britcher, Mehran Ghofrani

Department of Mechanical Engineering and Mechanics, Old Dominion University

7N-01-1R

8619

P 19

Abstract

A linearized dynamic model is developed for the Large-Angle Magnetic Suspension Test Fixture, a laboratory-scale magnetic suspension device under development at NASA Langley Research Center. The model follows outlines already established for the suspension elements, but is extended to include the analog controller and eddy current effects. Complete numerical data and some experimental validations are included.

List of Matrices (used in State-Space representations)

Open-Loop Dynamic Models

$\mathcal{AW}_2, \mathcal{BW}_2, \mathcal{C}, \mathcal{D}$	- Open-loop suspended element.
\mathcal{A}, \mathcal{B}	- $\mathcal{AW}_2, \mathcal{BW}_2$ prior to mass and inertia weighting.
$\mathcal{A}_{coil}, \mathcal{B}_{cmix}, \mathcal{C}_{coil}, \mathcal{D}_{coil}$	- Open-loop power supply/coil combination.
\mathcal{B}_{coil}	- \mathcal{B}_{cmix} prior to addition of demand allocation matrix.
$\mathcal{A}_c, \mathcal{B}_c, \mathcal{C}_c, \mathcal{D}_c$	- Single dual phase-advance compensator.
$\mathcal{AA}_c, \mathcal{BB}_c, \mathcal{CC}_c, \mathcal{DD}_c$	- Five parallel dual-phase advance compensators.
$\mathcal{CC}_g, \mathcal{DD}_g$	- Compensators with gain matrix added.
$\mathcal{A}_e, \mathcal{B}_e, \mathcal{C}_e, \mathcal{D}_e$	- Eddy current effect of field on model.

Connected Elements

$\mathcal{A}_p, \mathcal{B}_p, \mathcal{C}_p, \mathcal{D}_p$	- Forward path of closed-loop system.
$\mathcal{A}_{fb}, \mathcal{B}_{fb}, \mathcal{C}_{fb}, \mathcal{D}_{fb}$	- Closed-loop system.

Miscellaneous

\mathcal{G}_n	- Gain matrix (terms on leading diagonal).
\mathcal{M}_{ix}	- Demand allocation matrix.
\mathcal{L}	- Coil inductance matrix
\mathcal{R}_K	- Resistance matrix, including current feedback

1. Introduction

As part of NASA program to demonstrate the magnetic suspension of objects over wide ranges of attitudes, a laboratory-scale research project has been undertaken, the Large-Angle Magnetic Suspension Test Fixture (LAMSTF). A cylindrical element containing a permanent magnet core is levitated above a planar array of electromagnets, permitting demonstration of stability and control in five degrees-of-freedom, and of controlled rotation of the model in one degree-of-freedom over a range of 360 degrees.

Since a significant portion of this research effort will focus on the development and validation of control approaches, dynamic models of the LAMSTF are required to assist in control system development. This report discusses and details the development of a relatively simple linearized dynamic model, implemented using MATLAB.

2. Hardware Description

Five, room temperature, copper electromagnets, with iron cores, are mounted in a circular array on a heavy aluminum plate. The suspended element consists of Neodymium-Iron-Boron permanent magnet material epoxied into an aluminum tube. The position sensing system features multiple infra-red light beams, arranged in two orthogonal planes, partially interrupted by the model. The complete sensor system is mounted on a framework which is initially fixed in one orientation relative to the suspension electromagnets. However, the design permits rotation of the framework about a vertical axis, by some form of drive to be added later. A schematic diagram of LAMSTF is shown in Figure 1. The analog controller includes position sensor decoding, dual series phase-advance compensators and extensive decoupling at the output of the controller. A block diagram of the controller is shown in Figure 2. Each electromagnet is driven by a transistor switching power amplifier. More extensive details of LAMSTF hardware can be found in Refs. 1,2.

3. Linear Modelling of LAMSTF

Figure 3 shows a block diagram representing the important dynamic elements of LAMSTF. A State-Space model of this system will be developed. More detailed dynamic features, such as eddy currents, will be discussed later.

3.1 "Plant" - (Suspended Element)

Following the theory and notation of Refs. 3,4, the linearized dynamics of the

suspended element, due to its interaction with the quasi-steady suspension fields, can be written as follows :

$$\{\dot{\delta X}\} = \mathcal{A} \{\delta X\} + \mathfrak{B} \{\delta I\}$$

$$\text{where } \{\delta X\}^T = \{ \Omega_{\bar{y}} \quad \Omega_{\bar{z}} \quad \theta_y \quad \theta_z \quad V_{\bar{x}} \quad V_{\bar{y}} \quad V_{\bar{z}} \quad x \quad y \quad z \}$$

$$\mathcal{A} = \mathcal{W}_2 \times \begin{bmatrix} 0 & 0 & -B_x & 0 & 0 & 0 & 0 & -B_{xz} & -B_{yz} & -B_{zz} \\ 0 & 0 & 0 & -B_x & 0 & 0 & 0 & B_{xy} & B_{yy} & B_{yz} \\ 0 & 0 & 0 & 0 & 0 & 0 & 0 & 0 & 0 & 0 \\ 0 & 0 & 0 & 0 & 0 & 0 & 0 & 0 & 0 & 0 \\ 0 & 0 & -B_{xz} & 2 B_{xy} & 0 & 0 & 0 & (B_{xx})_x & (B_{xx})_y & (B_{xx})_z \\ 0 & 0 & B_{yz} & (B_{yy} - B_{xx}) & 0 & 0 & 0 & (B_{xy})_x & (B_{xy})_y & (B_{xy})_z \\ 0 & 0 & (B_{xx} - B_{zz}) & B_{yz} & 0 & 0 & 0 & (B_{xz})_x & (B_{xz})_y & (B_{xz})_z \\ 0 & 0 & 0 & 0 & 0 & 0 & 0 & 0 & 0 & 0 \\ 0 & 0 & 0 & 0 & 0 & 0 & 0 & 0 & 0 & 0 \\ 0 & 0 & 0 & 0 & 0 & 0 & 0 & 0 & 0 & 0 \end{bmatrix}$$

$$\text{and } \mathcal{W}_2 = \text{Vol} \times M_{\bar{x}} \begin{bmatrix} \frac{1}{I_c} & & & & & & & & & \\ & \frac{1}{I_c} & 0 & & & & & & & \\ & & 0 & & & & & & & \\ & & & 0 & & & & & & \\ & & & & \frac{1}{m_c} & & & & & \\ & & & & & \frac{1}{m_c} & & & & \\ & & & & & & \frac{1}{m_c} & & & \\ & & & & & & & 0 & & \\ & & & & & & & & 0 & \\ & & & & & & & & & 0 \end{bmatrix}$$

$$\mathfrak{B} = \frac{1}{I_{\max}} \mathcal{W}_2 \times \begin{bmatrix} -K_{z1} & -K_{z2} & -K_{z3} & -K_{z4} & -K_{z5} \\ K_{y1} & K_{y2} & K_{y3} & K_{y4} & K_{y5} \\ & & \dots 0 \dots \\ & & \dots 0 \dots \\ K_{xx1} & K_{xx2} & K_{xx3} & K_{xx4} & K_{xx5} \\ K_{xy1} & K_{xy2} & K_{xy3} & K_{xy4} & K_{xy5} \\ K_{xz1} & K_{xz2} & K_{xz3} & K_{xz4} & K_{xz5} \\ & & \dots 0 \dots \\ & & \dots 0 \dots \\ & & \dots 0 \dots \end{bmatrix}$$

In the particular case of LAMSTF, the numerical values of \mathcal{A} , \mathcal{W}_2 and $(\mathcal{B} \cdot \mathcal{W}_2 / I_{\max})$ are found to be (see also Appendix A) :

$$\mathcal{A} = \mathcal{W}_2 \times \begin{bmatrix} 0 & 0 & 7.8466e-3 & 0 & 0 & 0 & 0 & -9.25e-2 & 0 & 0 \\ 0 & 0 & 0 & 7.8466e-3 & 0 & 0 & 0 & 0 & 0 & 0 \\ 0 & 0 & 0 & 0 & 0 & 0 & 0 & 0 & 0 & 0 \\ 0 & 0 & 0 & 0 & 0 & 0 & 0 & 0 & 0 & 0 \\ 0 & 0 & -9.25e-2 & 0 & 0 & 0 & 0 & 4.7101e-1 & 0 & -2.3664e-4 \\ 0 & 0 & 0 & 0 & 0 & 0 & 0 & 0 & 9.0149e-1 & 0 \\ 0 & 0 & 0 & 0 & 0 & 0 & 0 & -2.3664e-4 & 0 & -8.6137e-3 \\ 0 & 0 & 0 & 0 & 0 & 0 & 0 & 0 & 0 & 0 \\ 0 & 0 & 0 & 0 & 0 & 0 & 0 & 0 & 0 & 0 \\ 0 & 0 & 0 & 0 & 0 & 0 & 0 & 0 & 0 & 0 \end{bmatrix}$$

$$\mathcal{W}_2 = \begin{bmatrix} 4.3308e5 & & & & & & & & & \\ & 4.3308e5 & & & & & & & & \\ & & 1 & & \dots & 0 & \dots & & & \\ & & & 1 & & & & & & \\ & & & & 1.0602e2 & & & & & \\ & & & & & 1.0602e2 & & & & \\ & & & & & & 1.0602e2 & & & \\ & & \dots & 0 & \dots & & & 1 & & \\ & & & & & & & & 1 & \\ & & & & & & & & & 1 \end{bmatrix}$$

$$\frac{\mathcal{B} \mathcal{W}_2}{I_{\max}} = \begin{bmatrix} 4.0710e1 & 4.0710e1 & 4.0710e1 & 4.0710e1 & 4.0710e1 \\ 0 & 9.5278e1 & 5.8899e1 & -5.8899e1 & -9.5278e1 \\ 0 & 0 & 0 & 0 & 0 \\ 0 & 0 & 0 & 0 & 0 \\ 2.3101e-1 & -1.5935e-1 & 8.1846e-2 & 8.1846e-2 & -1.593e-1 \\ 0 & 1.268e-1 & -2.0525e-1 & 2.0525e-1 & -1.268e-1 \\ -2.8869e-1 & -8.9161e-2 & 2.3356e-1 & 2.3356e-1 & -8.9161e-2 \\ 0 & 0 & 0 & 0 & 0 \\ 0 & 0 & 0 & 0 & 0 \\ 0 & 0 & 0 & 0 & 0 \end{bmatrix}$$

The eigenvalues and eigenvectors of matrix $\mathcal{A}W_2$ are as follows :

Mode 1 - 59.26 rad/s	Unstable divergence	x, θ_y	Axial + pitch
Mode 2 - 7.972	Stable oscillatory	x, θ_y	Axial + pitch
Mode 3 - 58.294	Unstable divergence	θ_z	Yaw rotation
Mode 4 - 0.956	Stable oscillatory	z	Vertical motion
Mode 5 - 9.776	Unstable divergence	y	Lateral translation

Modes 1 and 3 are referred to as the “compass needle” modes, since they arise from the tendency of the suspended element to reverse its direction in the applied axial field, B_x . They are the most important from the control point of view, since they have the highest unstable natural frequencies, close to 10Hz here. The mode shapes broadly correspond to the solutions for larger systems given in Ref. 4.

3.2 Power Supply / Electromagnets

The resistance and inductance of the LAMSTF electromagnets have been measured using standard instruments. The results are shown in Appendix A. There is some difficulty in specifying the inductance due to eddy currents in the aluminum baseplate and the (solid) iron electromagnet cores, as discussed more fully in Refs. 1,2.

The terminal voltage of a single electromagnet, inductively coupled to others, can be written :

$$V_1 = I_1 (R_1 + L_1 s) + I_2 L_{12} s + I_3 L_{13} s + \dots$$

An array of five electromagnets can thus be represented by the single equation :

$$\begin{bmatrix} L_1 & L_{12} & L_{13} & L_{14} & L_{15} \\ L_{21} & L_2 & L_{23} & L_{24} & L_{25} \\ L_{31} & L_{32} & L_3 & L_{34} & L_{35} \\ L_{41} & L_{42} & L_{43} & L_4 & L_{45} \\ L_{51} & L_{52} & L_{53} & L_{54} & L_5 \end{bmatrix} \begin{bmatrix} \bullet \\ I_1 \\ I_2 \\ I_3 \\ I_4 \\ I_5 \end{bmatrix} = - \begin{bmatrix} R_1 & 0 & 0 & 0 & 0 \\ 0 & R_2 & 0 & 0 & 0 \\ 0 & 0 & R_3 & 0 & 0 \\ 0 & 0 & 0 & R_4 & 0 \\ 0 & 0 & 0 & 0 & R_5 \end{bmatrix} \begin{bmatrix} I_1 \\ I_2 \\ I_3 \\ I_4 \\ I_5 \end{bmatrix} + \begin{bmatrix} V_1 \\ V_2 \\ V_3 \\ V_4 \\ V_5 \end{bmatrix}$$

The LAMSTF power amplifiers are presumed to resemble a voltage amplifier with current feedback, as shown in Figure 4. The input voltage to load current transfer function in this case is :

$$\frac{I}{V_D} = \frac{K}{R + Kk} * \frac{1}{1 + \left(\frac{L}{R + Kk}\right)s}$$

Thus the state-space equation may be modified as follows :

$$\begin{bmatrix} L_1 & L_{12} & L_{13} & L_{14} & L_{15} \\ L_{21} & L_2 & L_{23} & L_{24} & L_{25} \\ L_{31} & L_{32} & L_3 & L_{34} & L_{35} \\ L_{41} & L_{42} & L_{43} & L_4 & L_{45} \\ L_{51} & L_{52} & L_{53} & L_{54} & L_5 \end{bmatrix} \begin{bmatrix} \dot{I}_1 \\ \dot{I}_2 \\ \dot{I}_3 \\ \dot{I}_4 \\ \dot{I}_5 \end{bmatrix} = - \begin{bmatrix} R_1 + Kk & 0 & 0 & 0 & 0 \\ 0 & R_2 + Kk & 0 & 0 & 0 \\ 0 & 0 & R_3 + Kk & 0 & 0 \\ 0 & 0 & 0 & R_4 + Kk & 0 \\ 0 & 0 & 0 & 0 & R_5 + Kk \end{bmatrix} \begin{bmatrix} I_1 \\ I_2 \\ I_3 \\ I_4 \\ I_5 \end{bmatrix} + K \times \begin{bmatrix} V_{1D} \\ V_{2D} \\ V_{3D} \\ V_{4D} \\ V_{5D} \end{bmatrix}$$

The values of K and k can be estimated by measuring the D.C. gain and break frequency of the amplifier/coil combination. These have been set and measured as 3 A/V and 180Hz respectively. It is easily shown that for these values K=93.33 and k=0.325. The state-space model becomes :

$$\begin{bmatrix} \dot{I}_1 \\ \dot{I}_2 \\ \dot{I}_3 \\ \dot{I}_4 \\ \dot{I}_5 \end{bmatrix} = \begin{bmatrix} -1.1377e3 & 6.4601e1 & 1.0092e1 & 1.0092e1 & 6.4601e1 \\ 6.4596e1 & -1.1376e3 & 6.4596e1 & 1.0091e1 & 1.0091e1 \\ 1.0091e1 & 6.4596e1 & -1.1376e3 & 6.4596e1 & 1.0091e1 \\ 1.0091e1 & 1.0091e1 & 6.4596e1 & -1.1376e3 & 6.4596e1 \\ 6.4596e1 & 1.0091e1 & 1.0091e1 & 6.4596e1 & -1.1376e3 \end{bmatrix} \begin{bmatrix} I_1 \\ I_2 \\ I_3 \\ I_4 \\ I_5 \end{bmatrix} + \begin{bmatrix} 3.4172e3 & -1.9404e2 & -3.0313e1 & -3.0313e1 & -1.9404e2 \\ -1.9404e2 & 3.4172e3 & -1.9404e2 & -3.0313e1 & -3.0313e1 \\ -3.0313e1 & -1.9404e2 & 3.4172e3 & -1.9404e2 & -3.0313e1 \\ -3.0313e1 & -3.0313e1 & -1.9404e2 & 3.4172e3 & -1.9404e2 \\ -1.9404e2 & -3.0313e1 & -3.0313e1 & -1.9404e2 & 3.4172e3 \end{bmatrix} \begin{bmatrix} V_{1D} \\ V_{2D} \\ V_{3D} \\ V_{4D} \\ V_{5D} \end{bmatrix}$$

3.3 Compensators

A dual phase-advance compensator is of the following form :

$$\frac{V_o}{V_i} = \left(\frac{1 + nTs}{1 + Ts} \right)^2$$

In LAMSTF, the factor n was set as 11.3 and T was chosen as 0.0013. Both parameters are thought to require some fine-tuning. A state-space model can be derived using a standard canonical form :

$$\mathcal{A}_c = \begin{bmatrix} -\frac{2}{T} & -\frac{1}{T^2} \\ 1 & 0 \end{bmatrix} \quad \mathcal{B}_c = \begin{bmatrix} 1 \\ 0 \end{bmatrix} \quad \mathcal{C}_c = \begin{bmatrix} \frac{2n}{T} - \frac{2n^2}{T} & \frac{1}{T^2} - \frac{n^2}{T^2} \end{bmatrix} \quad \mathcal{D}_c = \begin{bmatrix} n^2 \end{bmatrix}$$

Using the values shown above, the model becomes :

$$\mathcal{A}_c = \begin{bmatrix} -1.5385e3 & -5.9172e5 \\ 1 & 0 \end{bmatrix} \quad \mathcal{B}_c = \begin{bmatrix} 1 \\ 0 \end{bmatrix} \quad \mathcal{C}_c = \begin{bmatrix} -1.7906e5 & -7.4964e7 \end{bmatrix} \quad \mathcal{D}_c = \begin{bmatrix} 127.69 \end{bmatrix}$$

Five independent compensators can be placed in parallel by using the MATLAB "APPEND" command.

3.4 Mixing

A mixing or decoupling matrix is included in order to distribute force and torque demands (in model degrees-of-freedom) amongst the five electromagnets. Initially, a basic matrix can be generated by solving for the current distribution required for 1 unit of field or field gradient of the appropriate type and sense. This gives :

$$\begin{bmatrix} I_{1D} \\ I_{2D} \\ I_{3D} \\ I_{4D} \\ I_{5D} \end{bmatrix} = \begin{bmatrix} 1.8282e3 & 0 & 1.9652e2 & 0 & -1.4687e2 \\ 2.3703e3 & 1.6446e3 & -1.5901e2 & 1.1553e2 & -4.5418e1 \\ 2.0347e3 & 1.016e3 & 6.0751e1 & -1.8689e2 & 1.1885e2 \\ 2.0347e3 & -1.016e3 & 6.0751e1 & 1.8689e2 & 1.1885e2 \\ 2.3703e3 & -1.6446e3 & -1.5901e2 & -1.1553e2 & -4.5418e1 \end{bmatrix} \begin{bmatrix} -B_z \\ B_y \\ B_{xx} \\ B_{xy} \\ B_{xz} \end{bmatrix}$$

In the analog controller, individual columns of the matrix were normalized to simplify manufacture :

$$\begin{bmatrix} I_{1D}' \\ I_{2D}' \\ I_{3D}' \\ I_{4D}' \\ I_{5D}' \end{bmatrix} = \begin{bmatrix} 0.7713 & 0 & 1 & 0 & -1 \\ 1 & 1 & -0.8091 & 0.6182 & -0.3092 \\ 0.8584 & 0.6178 & 0.3091 & -1 & 0.8092 \\ 0.8584 & -0.6178 & 0.3091 & 1 & 0.8092 \\ 1 & -1 & -0.8091 & -0.6182 & -0.3092 \end{bmatrix} \begin{bmatrix} -B_z \\ B_y \\ B_{xx} \\ B_{xy} \\ B_{xz} \end{bmatrix}$$

This results in a residual gain matrix being effectively incorporated into the decoupler, where the coefficients are the normalizing factors :

$$\begin{bmatrix} I_{1D} \\ I_{2D} \\ I_{3D} \\ I_{4D} \\ I_{5D} \end{bmatrix} = \begin{bmatrix} 2.3703e3 & 0 & 0 & 0 & 0 \\ 0 & 1.6446e3 & 0 & 0 & 0 \\ 0 & 0 & 1.9652e2 & 0 & 0 \\ 0 & 0 & 0 & 1.8689e2 & 0 \\ 0 & 0 & 0 & 0 & 1.4687e2 \end{bmatrix} \begin{bmatrix} I_{1D}' \\ I_{2D}' \\ I_{3D}' \\ I_{4D}' \\ I_{5D}' \end{bmatrix}$$

In fact, a slightly different (earlier) set of field coefficients were used to calculate the decoupling matrix actually implemented in hardware. Only the first column differs significantly from that shown above :

$$\begin{bmatrix} I_{1D}' \\ I_{2D}' \\ I_{3D}' \\ I_{4D}' \\ I_{5D}' \end{bmatrix} = \begin{bmatrix} 0.625 & 0 & 1 & 0 & -1 \\ 1 & 1 & -0.809 & 0.618 & -0.309 \\ 0.768 & 0.618 & 0.309 & -1 & 0.809 \\ 0.768 & -0.618 & 0.309 & 1 & 0.809 \\ 1 & -1 & -0.809 & -0.618 & -0.309 \end{bmatrix} \begin{bmatrix} -B_z \\ B_y \\ B_{xx} \\ B_{xy} \\ B_{xz} \end{bmatrix}$$

3.5 Eddy Current Effects

It has been found that the terminal characteristics of the electromagnets are significantly affected by the induction of eddy currents into the aluminum mounting plate and the solid iron electromagnet cores [2]. A simple analysis, assuming that the eddy current circuit is independent of frequency (implying that the skin depth \gg material thickness; also referred to in the literature as the Single Time Constant Model), gives a terminal voltage to current transfer function of :

$$\frac{I}{V} = \left(\frac{1}{(R + Ls) - \frac{(L_{m1}s)^2}{R_{e1} + L_{e1}s} - \dots} \right)$$

where R_{en} , L_{en} are the resistance and inductance of the n 'th eddy current circuit and L_{mn} is the mutual inductance between the primary (the electromagnet coil) and the eddy current circuit. The demand voltage to current transfer function is :

$$\frac{I}{V_D} = \left(\frac{K}{((R + Kk) + Ls) - \frac{(L_{m1}s)^2}{R_{e1} + L_{e1}s} - \dots} \right)$$

Continuing, the field components generated (at the suspended object) can be expressed as :

$$B = K_B I \left(1 - \frac{K_{e1} L_{m1} s}{K_B (R_{e1} + L_{e1}s)} - \dots \right) = K_B I + K_{e1} I_{e1} + \dots$$

where K_B , K_{en} are constants representing the field generated at the suspension location by the electromagnet and the n 'th eddy current respectively. Now the factor K_{en} will, in general, be different for each field component (see Section 3.1, \mathfrak{B} matrix). Here, for simplicity, it has been assumed that the ratio (K_{en}/K_B) will be equal for all components, since the eddy currents physically occur in circuits close to the suspension electromagnets. This permits modelling of the eddy current influence by invoking a false current :

$$I' = \left(1 - \frac{K_{e1} L_{m1} s}{K_B (R_{e1} + L_{e1}s)} + \dots \right) I, \quad \text{where } B = K_B I'$$

It should be noted that the change in terminal characteristics and the change in field at the model are two separate effects and should be modelled as such.

It has been argued that the factors K_{en} , L_{en}/R_{en} and L_{mn} can be estimated by geometrical analysis and by careful measurements of electromagnet terminal characteristics. Results are given in Appendix A. So far, it has not been possible to express the change in terminal characteristics in an elegant generic state-space form.

However, numerical results for LAMSTF, using results from Appendix A are as follows :

$$\mathcal{A} = \begin{bmatrix} -1.2548e5 & -1.4037e8 \\ 1 & 0 \end{bmatrix} \quad \mathfrak{B} = \begin{bmatrix} 1 \\ 0 \end{bmatrix} \quad \mathcal{C} = \begin{bmatrix} 7.459e3 & 9.8385e5 \end{bmatrix} \quad \mathfrak{D} = \begin{bmatrix} 0 \end{bmatrix}$$

- where only the eddy current in the aluminum plate is considered. In fact, analysis has indicated that the eddy current in the iron core has negligible effect on system dynamics, partly due to the high resonant frequency involved (R_e/L_e).

The change in field at the suspended element due to the eddy currents can be represented by parallel state-space models, where each model represents one eddy current. The equations relating the actual current to the fictitious current I' , for one eddy current circuit, again using a standard canonical form, can be written:

$$\mathcal{A}_e = \begin{bmatrix} -\frac{R_e}{L_e} \end{bmatrix} \quad \mathfrak{B}_e = \begin{bmatrix} 1 \end{bmatrix} \quad \mathcal{C}_e = \begin{bmatrix} \frac{K_e L_m R_e}{K_B L_e^2} \end{bmatrix} \quad \mathfrak{D}_e' = \begin{bmatrix} -\frac{K_e L_m}{K_B L_e} \end{bmatrix}$$

To integrate this model into the basic system, the \mathfrak{D}_e' matrix must be modified slightly, so as to carry the primary $B = K_B I$ term :

$$\mathfrak{D}_e = \begin{bmatrix} 1 - \frac{K_e L_m}{K_B L_e} \end{bmatrix}$$

Additional parallel eddy current circuits could be incorporated using the MATLAB "PARALLEL" command, but again, analysis has indicated that only the eddy current in the aluminum plate has a significant effect on system dynamics.

4. Comparison of Model to Hardware

The measured sensitivities of the position sensors, around the normal operating point, are as follows :

Sensor	Function	Sensitivity (V/m)
1	Aft vertical	4232
2	Axial	3693
3	Forward vertical	6079
4	Aft lateral	5929
5	Forward lateral	2748

These figures are subject to considerable variation depending on precise alignment and focusing of the sensors optics. Therefore, it seems reasonable to use an average sensitivity for further calculations.

$$\overline{\text{Sensitivity}} = 4536 \text{ V/m}$$

The fore-and-aft spacing of beams 1 and 3 is 0.0317m and of beams 4 and 5 is 0.0349m, leading to angular sensitivities in pitch and yaw of 143.8 V/rad and 158.3 V/rad respectively.

Representative gain settings for the analog controller, qualitatively found to give good damping in all degrees-of-freedom are :

Degree-of-Freedom	Controller gain
Pitch (θ_y)	0.153 V/V
Yaw (θ_z)	0.134
Axial (x)	0.2
Lateral (y)	0.203
Vertical (z)	0.548

Thus the overall system gains, measured from physical motion to the input to the decoupling matrix, are :

Degree-of-Freedom	Overall gain
Pitch (θ_y)	22.0 V/rad
Yaw (θ_z)	21.2 V/rad
Axial (x)	907.2 V/m
Lateral (y)	1841.6 V/m
Vertical (z)	4971.5 V/m

All other parts of the hardware are specifically modelled in the simulation.

Implementing these physical gain values in the simulation, the G_n matrix becomes:

N

$$G_n = \begin{bmatrix} 22 & 0 & 0 & 0 & 0 \\ 0 & 21.1 & 0 & 0 & 0 \\ 0 & 0 & 907.2 & 0 & 0 \\ 0 & 0 & 0 & 1841.6 & 0 \\ 0 & 0 & 0 & 0 & 4971.5 \end{bmatrix}$$

It is then easily confirmed that the resulting system is stable and has adequate damping and response in all controlled degrees-of-freedom, as illustrated in Figure 5.

5. Discussion

The general outline of the dynamic model presented here is thought to be reasonably valid insofar as it qualitatively reproduces observed behaviour, such as the coupling between pitch rotation and axial translation degrees-of-freedom. However, some of the numerical values presented are not exact. Most notably, there is a known discrepancy between the calculated equilibrium suspension currents and those measured in practice (the former being around 10% less than the latter). It is strongly suspected that the magnetization of the magnetic core of the suspended element is less than anticipated (i.e. less than 1.2 Tesla). Unfortunately, an accurate measurement of this quantity is quite difficult.

Acknowledgements

This work was supported by NASA Grant NAG-1-1056, Technical Monitor, Nelson J. Groom.

References

1. Britcher, C.P.; Ghofrani, M.; Britton, T.; Groom, N.J.: The Large-Angle Magnetic Suspension Test Fixture. International Symposium on Magnetic Suspension Technology. NASA Langley Research Center, August 1991. NASA CP-
2. Britcher, C.P.; Ghofrani, M.; Haj, A.; Britton, T.: Analysis, Modelling and Simulation of the Large-Angle Magnetic Suspension Test Fixture. ROMAG '92.
3. Groom, N.J.: Analytical Model of a Five Degree of Freedom Magnetic Suspension and Positioning System. NASA TM-100671, March 1989.
4. Groom, N.J.; Britcher, C.P.: Open-Loop Behaviour of Magnetic Suspension Systems Using Electromagnets Mounted in a Planar Array. NASA TP-

[Handwritten signature]

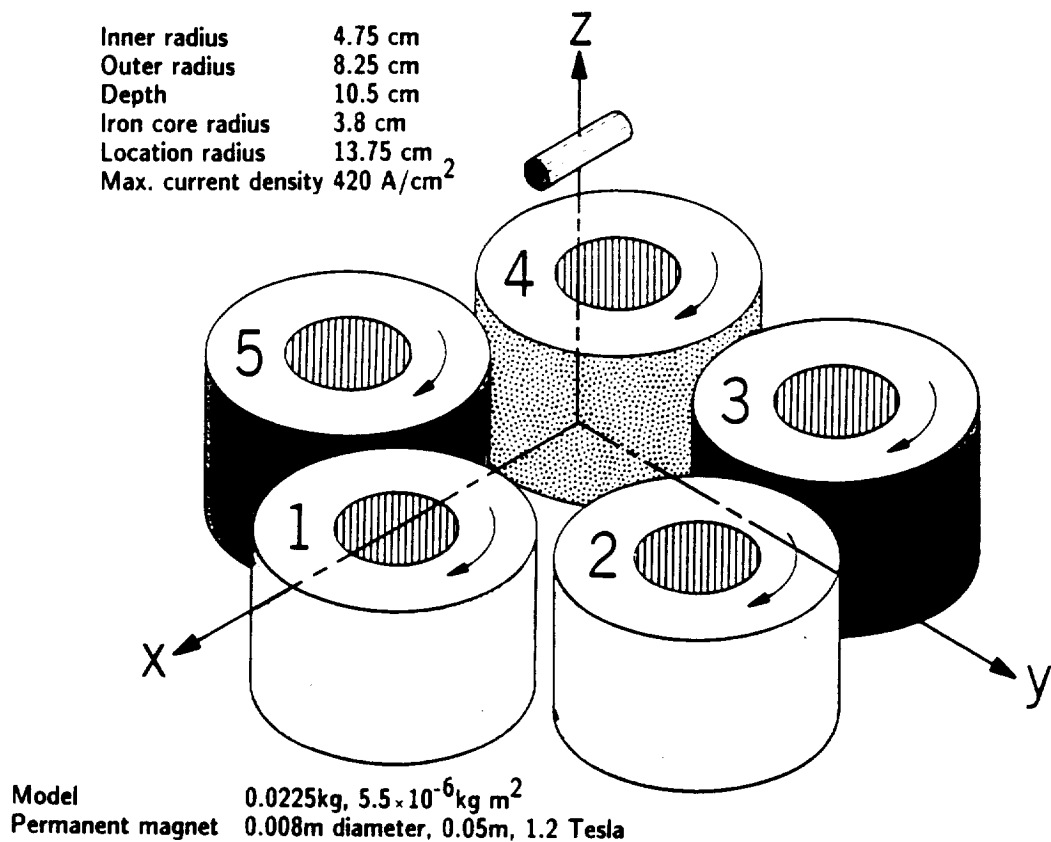


Figure 1 - Large-Angle Magnetic Suspension Test Fixture (LAMSTF) Configuration

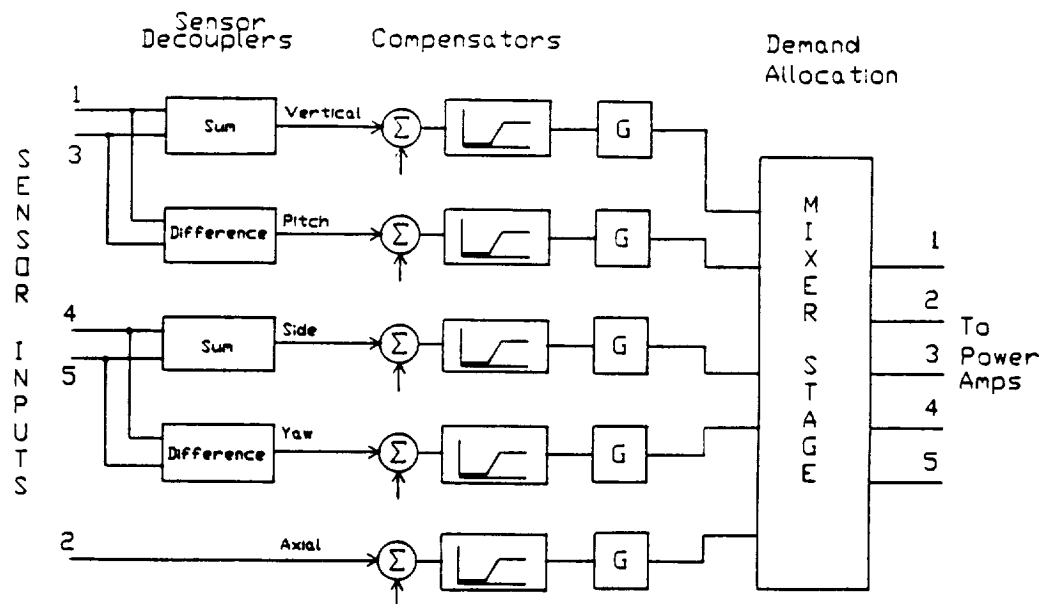


Figure 2 - Analog Controller Block Diagram

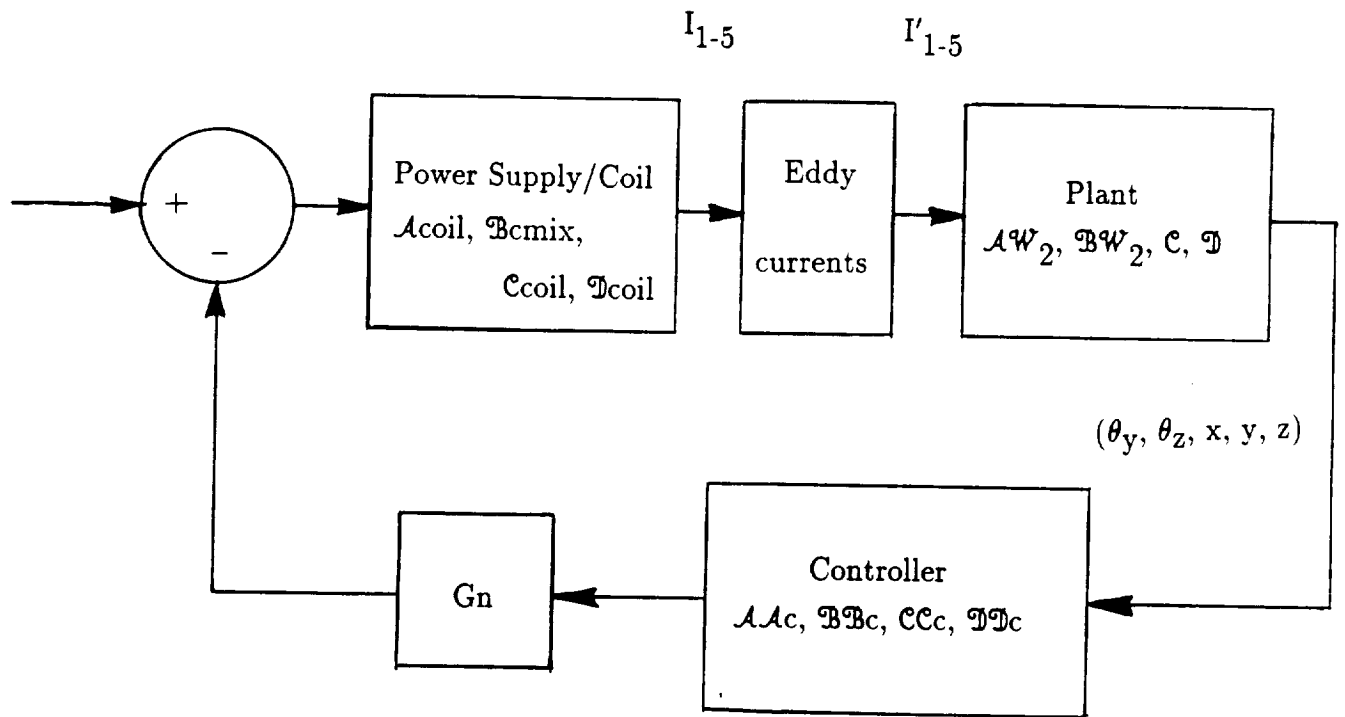


Figure 3 - Block Diagram of Essential Dynamics of LAMSTF

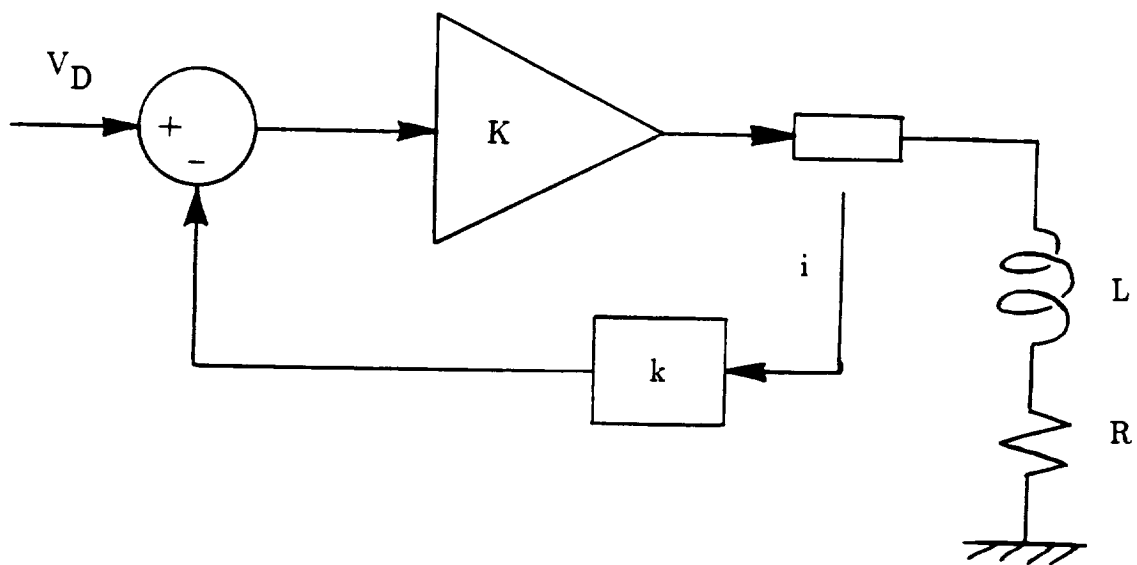


Figure 4 - Block Diagram of Power Supply/Coils

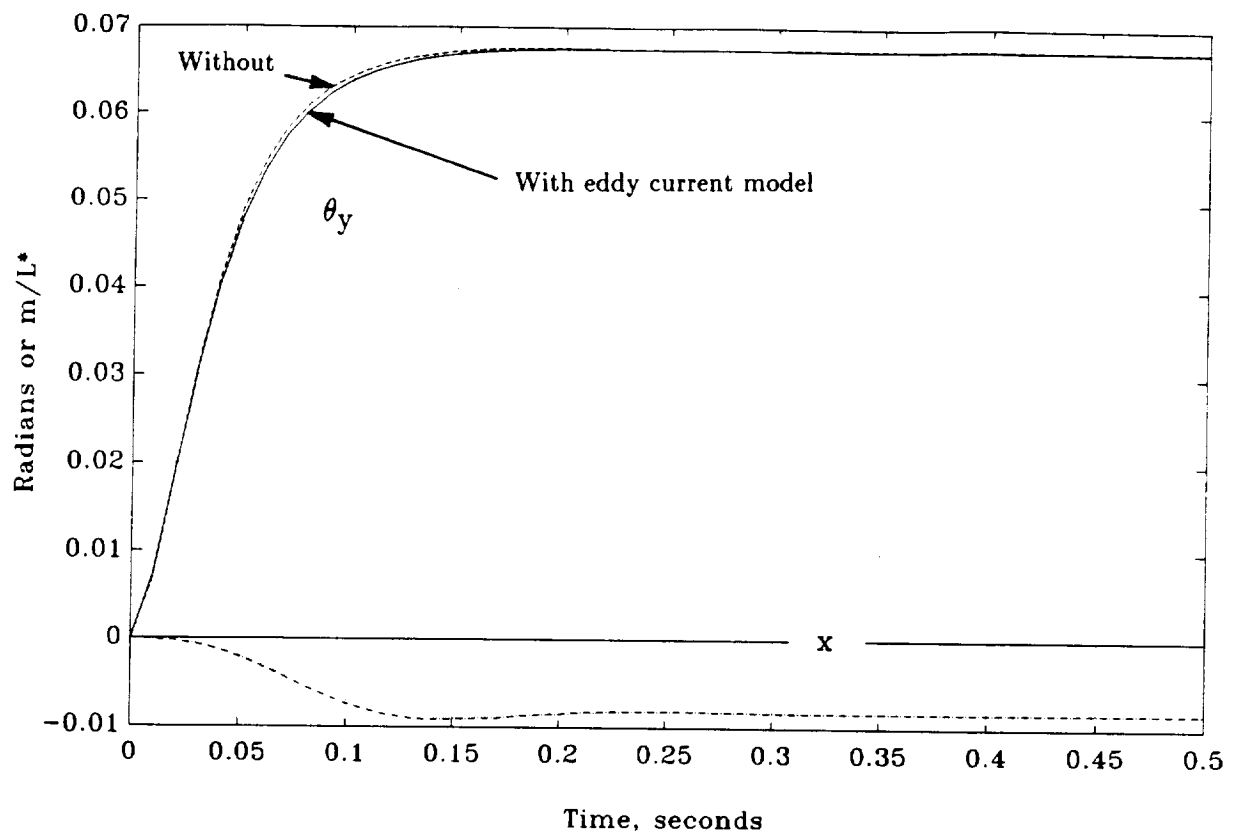


Figure 5a - Pitch (θ_y) Step Response of Simulated System

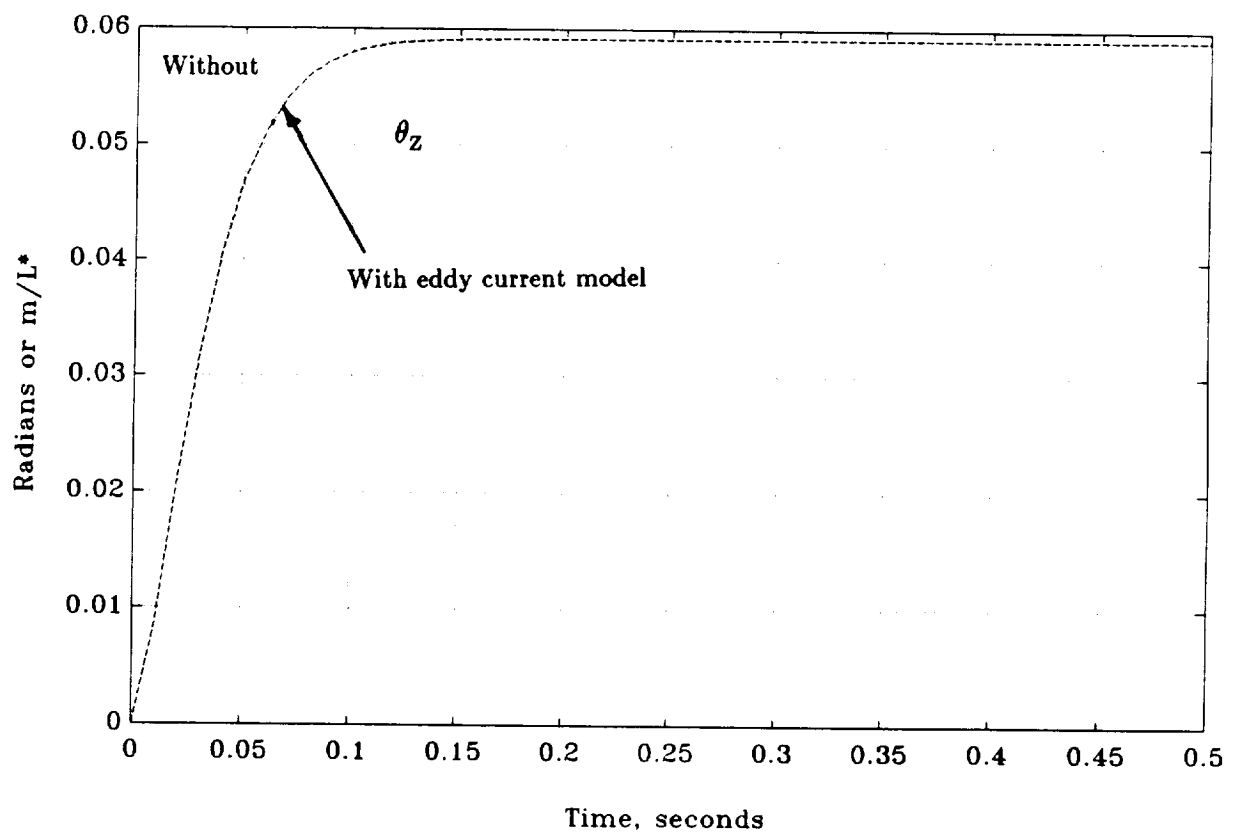


Figure 5b - Yaw (θ_z) Step Response of Simulated System

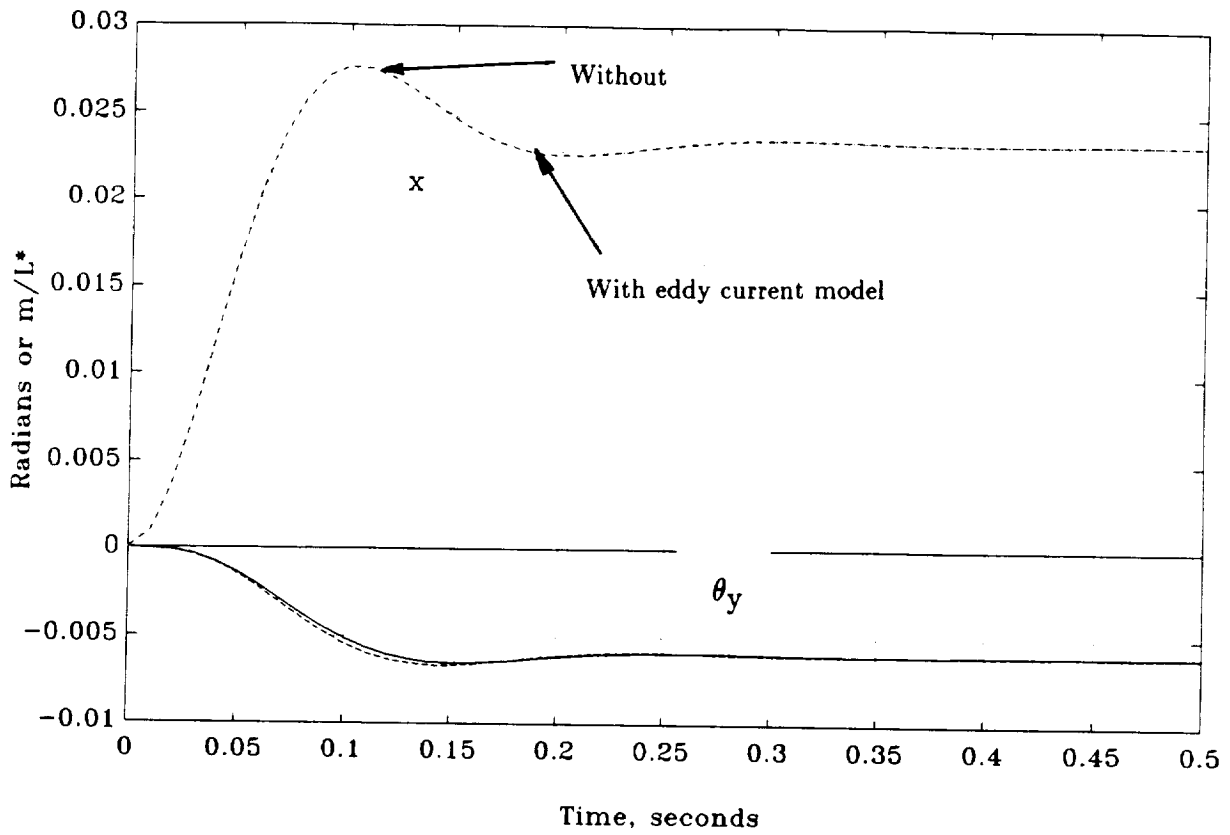


Figure 5c - Axial (x) Step Response of Simulated System

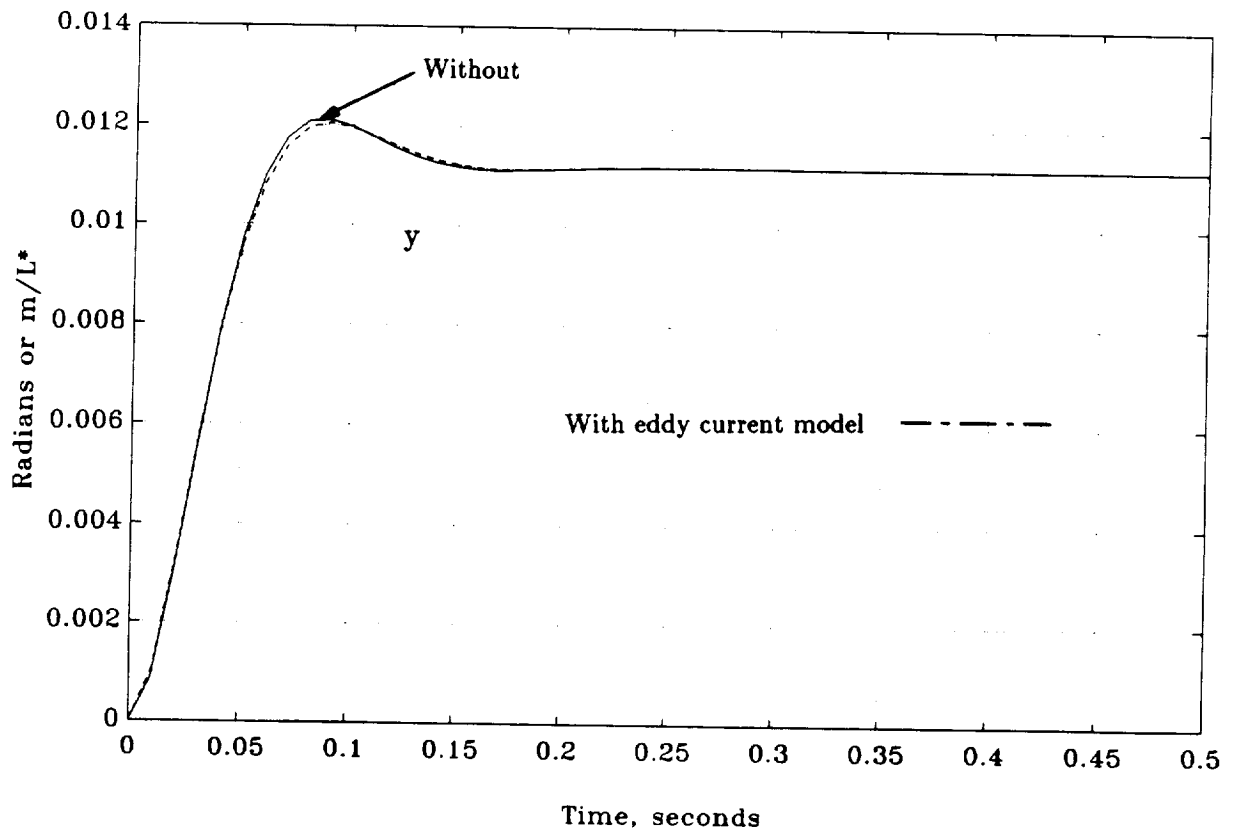


Figure 5d - Side (y) Step Response of Simulated System

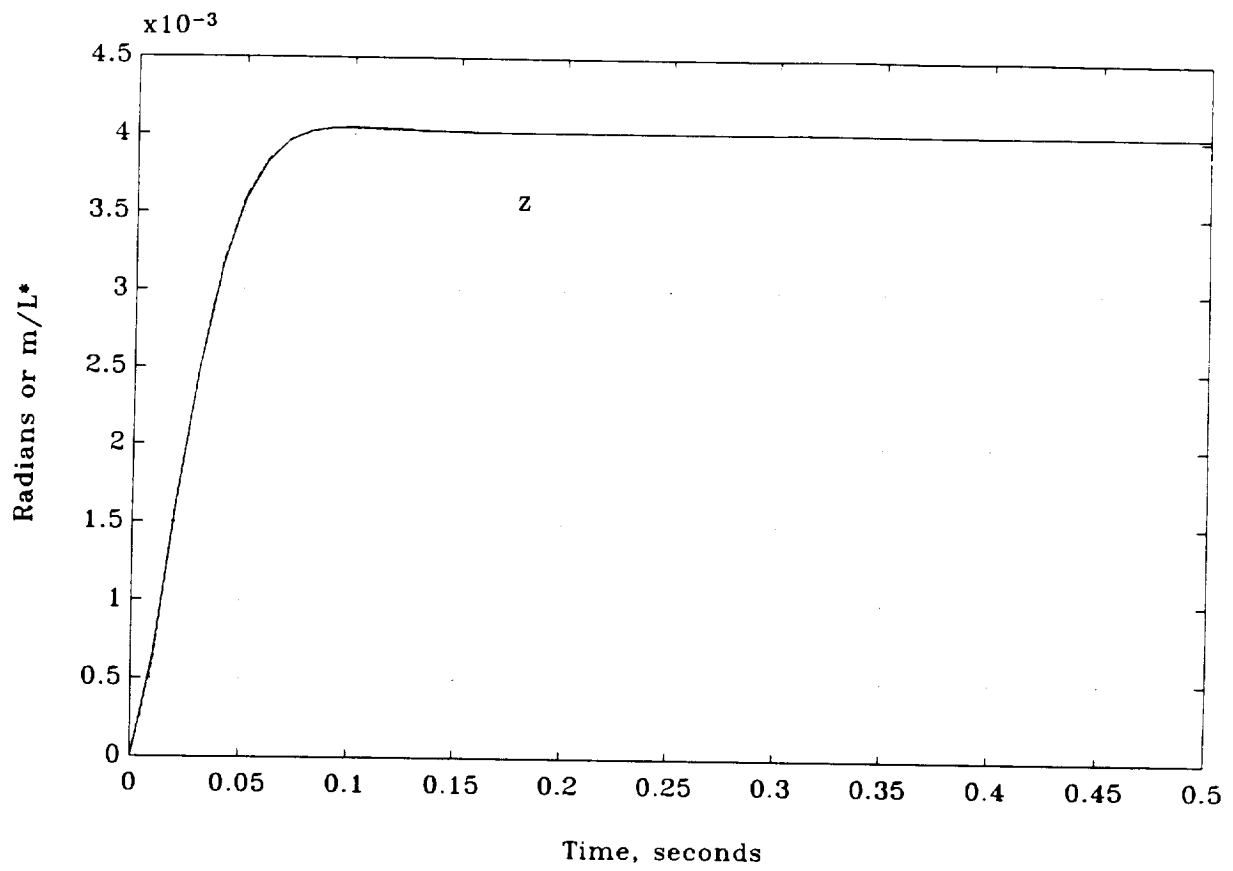


Figure 5e - Vertical (z) Step Response of Simulated System

APPENDIX A - LAMSTF Specifications

Field Coefficients (K_i), per Ampere

Coil #	B_x	B_y	B_z	B_{xx}	B_{xy}	$B_{xz} \times 10^6$
1	231	0	-94	2179	0	-2723
2	71	220	-94	-1503	1196	-841
3	-187	136	-94	772	-1936	2203
4	-187	-136	-94	772	1936	2203
5	71	-220	-94	-1503	-1196	-841

Coil #	B_{yy}	B_{yz}	B_{zz}	B_{xx_x}	B_{xxy}	$B_{xx_z} \times 10^6$
1	-1892	0	-287	3434	0	-53466
2	1790	-2590	-287	-18276	-14560	16371
3	-485	-1600	-287	16559	13733	-26790
4	-485	1600	-287	16559	-13733	-26790
5	1790	2590	-287	-18276	14560	16371

Coil #	B_{xyy}	B_{xyz}	B_{xzz}	B_{yyy}	B_{yyz}	B_{yzz}	$B_{zz_z} \times 10^6$
1	-21916	0	254	0	23744	0	295
2	-11938	8735	78	4944	50628	242	295
3	22896	-14134	-205	9129	34013	149	295
4	22896	14134	-205	-9129	34013	-149	295
5	-11938	-8735	78	-4944	50628	-241	295

All shown in T, T/m or T/m/m, per Ampere, times 10^6 . Calculated using VF/GFUN, including OPERA, with all iron cores modelled, using cartesian polynomial fitting of field at grid points.

Equilibrium conditions

$$I_0 = \{ -13.586, -4.201, 10.994, 10.994, -4.201 \} \text{ A ; } I_{\text{max}} = 30\text{A}$$

Significant uncontrolled fields with I_0 as shown above, T, T/m and T/m/m :

$$\begin{aligned} B_x &= -7.8466\text{e-}3 & B_{xx_x} &= 4.7101\text{e-}1 & B_{xx_z} &= -2.3664\text{e-}4 \\ B_{xy_y} &= 9.0149\text{e-}1 & B_{xz_z} &= -8.6137\text{e-}3 \end{aligned}$$

$$(B_{xz} \text{ required} = 0.0925 \text{ T/m})$$

Suspended element

$$\begin{aligned} m_c &= 22.5\text{e-}3 \text{ kg} & I_c &= 5.508\text{e-}6 \text{ kg m}^2 & \text{Vol} &= 2.498\text{e-}6 \text{ m}^3 \\ M_x &= 954930 \text{ A/m (1.2T)} & (g &= 9.80665 \text{ m/s}^2) \end{aligned}$$

$$\text{Characteristic length} = 0.02\text{m (Actual length} = 0.02095\text{m)}$$

Electromagnets

$$\begin{aligned} L &= 0.0275 \text{ H} & R &= 0.74 \Omega & N &= 509 \text{ turns} \\ L_{\text{mutual adjacent}} &= 0.0016 \text{ H} & L_{\text{mutual non-adjacent}} &= 0.00037 \text{ H} \end{aligned}$$

Eddy current circuits

The eddy circuit inductance is estimated by simple scaling laws, based on the measured inductance of the electromagnet itself. The resistance of the secondary is then adjusted to match the measured time constant. The mutual inductance is then adjusted to match the measured peak magnitude of phase defect.

Aluminum plate

$$L_{e1} = 1.0614\text{e-}7 \text{ H} \quad R_{e1} = 1.4\text{e-}5 \Omega \quad L_{m1} = 2.701\text{e-}5 \text{ H} \quad (0.5*\sqrt{(LL_{e1})})$$

$$\frac{K_{e1}}{K_B} = 1.1\text{e-}3 \quad (\text{including a factor accounting for magnetization of the iron cores})$$

Iron core

$$L_{e2} = 5.307\text{e-}8 \text{ H} \quad R_{e2} = 6\text{e-}3 \Omega \quad L_{m2} = 1.1461\text{e-}5 \text{ H} \quad (0.3*\sqrt{(LL_{e2})})$$

$$\frac{K_{e2}}{K_B} = 6.2\text{e-}6 \quad (\text{as above})$$